Null Broadening Robust Beamforming Based on Decomposition and Iterative Second-order Cone Programming

Wei JIN [1,2], Yunzhou GUO [2], Weimin JIA [2], Jianwei ZHAO [2]

[1] National Laboratory of Radar Signal Processing, Xidian University, Xi'an, 710071, China
[2] Xi'an Research Institute of High Technology, Hongqing Town, Xi'an, 710025, China

jinweimail@126.com, mailguoyunzhou@163.com, jwm602@163.com, zhaojianweiep@163.com

Submitted October 19, 2020 / Accepted August 25, 2021

Abstract. *To solve the problem that the performance of adaptive beamformer degrades severely in the presence of steering vector mismatch or non-stationary interference, a null broadening robust beamforming based on decomposition and iterative second-order cone programming (SOCP) is proposed. The width and depth of the nulls is controlled. The magnitude response constraints are applied to control the beamwidth and ripple of mainlobe, so the SV mismatch can be overcome. Due to the decomposition of the non-convex magnitude response constraints, the proposed approach can be solved by decomposition and iterative SOCP. Simulation results show that the proposed approach can effectively broaden the null width and enhance the null depth, and it is also robust against SV mismatch, especially large SV mismatch. The proposed approach is jointly robust against the SV mismatch and non-stationary interference, and is still effective in the case of low snapshot, which enhances the robustness of adaptive beamformer in complex environments.*

Keywords

Robust adaptive beamforming, null broadening, magnitude response constraints, second-order cone programming, joint robustness

1. Introduction

Adaptive beamforming is a classic problem in array signal processing and has been widely applied in radar, sonar, communications, microphone array processing, medical imaging and other fields [1]. The adaptive beamforming can enhance the desired signal (DS) and suppress the interferences as well as noise by adaptively adjusting the weight vectors of the array according to the received signal [2]. The traditional adaptive beamforming approaches are based on the ideal model in which the steering vector (SV) is accurately known and the DS components are not present in the received data. However, in practical situations, if there is signal SV mismatch due to signal look direction error, array location error and mutual coupling effect of array sensors, etc., the performance degradation of adaptive beamforming will occur [3], [4]. On the other hand, in most of applications, the DS components usually exist in the training data. In this case, a slight mismatch will also cause a serious degradation in the performance of adaptive beamforming. A series of robust adaptive beamforming algorithms against SV mismatch and covariance matrix estimation inaccuracy have been proposed, such as the diagonal loading (DL) technique [5], the eigenspace-based (EIG) beamformer [6], the robust adaptive beamforming based on the uncertainty set of SV [4], [7], the interference-plus-noise covariance matrix (INCM) reconstruction approach [8] and methods in [9], [10].

However, in many applications, there exists non-stationary interference that adaptive beamforming is also sensitive to. The nulls generated by the general adaptive beamformers are very sharp and narrow, which means that the interference can only be suppressed when it is strictly on the null position. When the interference moves quickly or the antenna platform vibrates, the update speed of adaptive weight vector may be slower than the speed of the interference, which will cause the mismatch between adaptive weight vector and data. At this time, the interference will move out of the null and cannot be suppressed effectively.

Null broadening is an effective method to suppress non-stationary interference and make it fall into the null. Covariance matrix tapers (CMT) [11–13] is a classic approach of null broadening. Mallioux [11] replaces the original single interference source with a cluster of incoherent and equal power virtual interference sources, and Zatman [12] uses a continuous interference source to replace the original single interference signal. Guerci [13] introduces the concept of CMT to unify them into one form. The CMT approach essentially utilizes a matrix related to null width to enhance the covariance matrix and broaden the nulls with low computational complexity. However, the CMT approach will cause higher sidelobe, shallower null depth, and smaller array gain. In [14], [15], the derivative con-

straint approach is proposed, which has been proved to be a form of the CMT approach by Zatman in [16]. A variety of null broadening methods based on optimization problems have been proposed in [17–20]. In [17], a null broadening beamformer based on multi-parameter quadratic programming is proposed, which constrains the null depth and sidelobe level on the basis of the CMT method. Quadratic constraint sector suppressed (QCSS) [18] controls the null depth by constraint, and its key idea is the array average output power on the interference angular sectors is lower than the pre-specified suppression level. However, it is too complicated to obtain the solution. In order to reduce the computational complexity, the original nonlinear quadratic constraint is replaced by a set of linear constraints, which is called linear constraint sector suppressed (LCSS) approach [19]. Mao et al. [20] propose a null broadening approach based on projection transformation and diagonal loading (PDL). It combines the CMT method and projection transformation, and the width and depth of its nulls are better than those of the CMT method's. The PDL approach has certain robustness to non-stationary interference and SV mismatch. In recent years, several null broadening methods based on covariance matrix reconstruction have been proposed [21], [22]. In [21], the nulls are imposed toward the angular sectors of the non-stationary interferences on the basis of INCM reconstruction. Meanwhile, similarity constraint is enforced to obtain well-maintained mainlobe of the beampattern. In [22], a reconstructed covariance matrix is derived from a simplified power spectral density function, and the nulls are broadened according to the direction of arrival (DOA) of the time-varying interference.

In this paper, we develop a null broadening robust beamforming algorithm based on decomposition and iterative second-order cone programming (NB-DISOCP). Firstly, a suppression level is set to make the array responses on the angular sectors of non-stationary interferences lower than it, so as to control the width and depth of nulls. And then the magnitude response constraints are applied to the mainlobe of the beam. The non-convex magnitude response constraint is decomposed, and the problem can be solved by iterative SOCP. The magnitude response constraint of the mainlobe can control the beamwidth and ripple of the mainlobe to overcome the SV mismatch. Moreover, the proposed algorithm combines the worst-case performance optimization (WCPO) method to correct the covariance matrix, which makes the estimation of the covariance matrix more accurate and improves the robustness of the proposed algorithm. Simulation results show that the proposed NB-DISOCP approach can effectively broaden the null width and enhance the null depth, and it is also robust against SV mismatch.

Our paper is organized as follows. In Sec. 2, the background of the adaptive beamforming is given. Our null broadening robust beamforming approach NB-DISOCP is introduced in Sec. 3. Section 4 presents our simulation results where the influence of parameters of the proposed NB-DISOCP is discussed and the performance of the proposed NB-DISOCP is compared with some existing algorithms. The conclusion is in Sec. 5.

2. Problem Background

Consider a uniform linear array of M omnidirectional sensors with the spacing of d, and assume that the received signals are far-field narrowband source signals. The received data of the array at time k can be modeled as [1]

$$\begin{aligned}\boldsymbol{x}(k) &= \boldsymbol{x}_{\mathrm{s}}(k) + \boldsymbol{x}_{\mathrm{i}}(k) + \boldsymbol{n}(k) \\ &= \boldsymbol{a}(\theta_0)s_0(k) + \sum_{i=1}^{M}\boldsymbol{a}(\theta_{\mathrm{i}})s_{\mathrm{i}}(k) + \boldsymbol{n}(k)\end{aligned} \tag{1}$$

where $\boldsymbol{x}_{\mathrm{s}}(k)$, $\boldsymbol{x}_{\mathrm{i}}(k)$, and $\boldsymbol{n}(k)$ denote the DS, interference, and noise components, respectively. $s_0(k)$ and $s_{\mathrm{i}}(k)$ are the DS waveform and interference signal waveform, respectively. Assume that the DS, interference, and noise are statistically independent narrowband Gaussian random processes. θ_0 and θ_{i} are the DOAs of the DS and the interference, respectively. $\boldsymbol{a}(\cdot)$ represents the $M \times 1$ dimensional signal SV, which can be written as

$$\boldsymbol{a}(\theta) = \left[1, \exp\left(-\mathrm{j}\frac{2\pi d \sin\theta}{\lambda}\right), \ldots, \exp\left(-\mathrm{j}\frac{2\pi(M-1)d\sin\theta}{\lambda}\right)\right]^{\mathrm{T}} \tag{2}$$

where λ is the wavelength, and $(\cdot)^{\mathrm{T}}$ denotes the transpose. The output of the narrowband adaptive beamformer is [1]

$$y(k) = \boldsymbol{w}^{\mathrm{H}}\boldsymbol{x}(k) \tag{3}$$

where $\boldsymbol{w} = [w_1, w_2, \ldots w_M]^{\mathrm{T}}$ is the $M \times 1$ dimensional adaptive weight vector.

Signal to interference plus noise ratio (SINR) is an important index to evaluate the performance of beamformer, which is the ratio of array output power of the desired signal to that of the interference-plus-noise [1]

$$\mathrm{SINR} = \frac{\sigma_{\mathrm{s}}^2\left|\boldsymbol{w}^{\mathrm{H}}\boldsymbol{a}(\theta_0)\right|^2}{\boldsymbol{w}^{\mathrm{H}}\boldsymbol{R}_{\mathrm{i+n}}\boldsymbol{w}} \tag{4}$$

where σ_{s}^2 is the desired signal power, $\boldsymbol{R}_{\mathrm{i+n}} = \mathrm{E}\{(\boldsymbol{x}_{\mathrm{i}}(k) + \boldsymbol{n}(k))(\boldsymbol{x}_{\mathrm{i}}(k) + \boldsymbol{n}(k))^{\mathrm{H}}\}$ is the $M \times M$ dimensional actual INCM, $\mathrm{E}\{\cdot\}$ is the statistical expectation, and $(\cdot)^{\mathrm{H}}$ is the Hermitian transpose. The adaptive weight vector of Capon beamformer is obtained by maximizing SINR, it can be written as [1]

$$\min_{\boldsymbol{w}} \boldsymbol{w}^{\mathrm{H}}\boldsymbol{R}_{\mathrm{i+n}}\boldsymbol{w}, \qquad \text{s.t.} \quad \boldsymbol{w}^{\mathrm{H}}\boldsymbol{a}(\theta_0) = 1. \tag{5}$$

The solution obtained from (5) is the Capon beamformer [1]

$$\boldsymbol{w}_{\mathrm{opt}} = \frac{\boldsymbol{R}_{\mathrm{i+n}}^{-1}\boldsymbol{a}(\theta_0)}{\boldsymbol{a}^{\mathrm{H}}(\theta_0)\boldsymbol{R}_{\mathrm{i+n}}^{-1}\boldsymbol{a}(\theta_0)}. \tag{6}$$

However, in practice, $\boldsymbol{R}_{\mathrm{i+n}}$ is unavailable, so the sample covariance matrix [1]

$$\hat{\boldsymbol{R}} = \frac{1}{N}\sum_{k=1}^{N} \boldsymbol{x}(k)\boldsymbol{x}^{\mathrm{H}}(k) \tag{7}$$

is frequently adopted to replace $\boldsymbol{R}_{\mathrm{i+n}}$, where N is the number of snapshots. And the corresponding beamformer is the sample matrix inversion (SMI) beamformer [1]

$$\boldsymbol{w}_{\mathrm{SMI}} = \frac{\hat{\boldsymbol{R}}^{-1}\boldsymbol{a}(\theta_0)}{\boldsymbol{a}^{\mathrm{H}}(\theta_0)\hat{\boldsymbol{R}}^{-1}\boldsymbol{a}(\theta_0)}. \tag{8}$$

3. The Proposed Algorithm

In this section, a null broadening robust beamforming algorithm NB-DISOCP based on decomposition and iterative second-order cone programming is proposed. The algorithm has joint robustness to SV mismatch and non-stationary interference. In the first subsection, the array responses on the angular sectors of non-stationary interferences are limited lower than the pre-specified suppression level to broaden the null width and control the null depth. In the second subsection, the magnitude response constraints are applied to the main lobe. The covariance matrix is estimated in the third subsection. The NB-DISOCP optimization problem and its solution as well as the complete algorithm steps are given in the fourth subsection.

3.1 Null Broadening

Assume that the interference signals impinge from the direction $\theta_p (p = 1,\ldots,P)$. When the interference moves rapidly, the incident directions of the interference signals are $\theta_k \in [\theta_p - \Delta\theta/2,\ \theta_p + \Delta\theta/2]$ $(k = 1,\ldots,K)$. Let the array response on the angular sectors of non-stationary interferences lower than the pre-specified suppression level ξ, such as

$$\left|\boldsymbol{w}^{\mathrm{H}}\boldsymbol{a}(\theta_k)\right| \le \xi,\ k = 1,\ldots,K. \tag{9}$$

3.2 Magnitude Response Constraints

In order to improve the robustness of the beamformer to the SV mismatch, the magnitude response constraints are applied to the angular region of the DS to form a flat-topped mainlobe, that is [10]

$$L \le \left|\boldsymbol{w}^{\mathrm{H}}\boldsymbol{a}(\theta)\right| \le U,\ \theta \in [\theta_L, \theta_U] \tag{10}$$

where U, L are the upper and lower limits of the magnitude constraint, respectively. θ_U, θ_L are the upper and lower limits of the angular region of the DS, respectively. All the signals in the region can be received, which reduces the sensitivity of the beamformer to the SV mismatch.

3.3 Covariance Matrix Estimation

In practical applications, the actual covariance matrix $\boldsymbol{R}$ is unavailable, so that the sample covariance matrix $\hat{\boldsymbol{R}}$ is usually used instead. As N increases, $\hat{\boldsymbol{R}}$ converges to $\boldsymbol{R}$. However, due to the limited number of snapshots, there exists mismatch between $\hat{\boldsymbol{R}}$ and $\boldsymbol{R}$. $\hat{\boldsymbol{R}}$ can be corrected by the WCPO method as [10]

$$\boldsymbol{R} = \hat{\boldsymbol{R}} + \boldsymbol{e} \tag{11}$$

where $\boldsymbol{e}$ is the mismatch vector between $\hat{\boldsymbol{R}}$ and $\boldsymbol{R}$. Its norm has an upper bound $\varepsilon > 0$ (ε is a constant), that is, $\|\boldsymbol{e}\| < \varepsilon$.

According to (5), the objective function can be written as [10]

$$\min_{\boldsymbol{w}} \max_{\|\boldsymbol{e}\|<\varepsilon} \boldsymbol{w}^{\mathrm{H}}(\hat{\boldsymbol{R}} + \boldsymbol{e})\boldsymbol{w} = \min_{\boldsymbol{w}} \boldsymbol{w}^{\mathrm{H}}(\hat{\boldsymbol{R}} + \varepsilon\boldsymbol{I})\boldsymbol{w}. \tag{12}$$

In practice, let $\varepsilon = \varepsilon_{\mathrm{r}}\,\hat{\boldsymbol{R}}(1,1)$ to enable ε to change with the input signal-to-noise ratio (SNR), where ε_{r} is a relative regularization factor, and $\hat{\boldsymbol{R}}(1,1)$ is the first row and the first column element of $\hat{\boldsymbol{R}}$ [10].

3.4 NB-DISOCP Beamformer

According to (5), (9), (10) and (12), the NB-DISOCP optimization problem can be written as

$$\begin{aligned} \min_{\boldsymbol{w}} \quad & \boldsymbol{w}^{\mathrm{H}}(\hat{\boldsymbol{R}} + \varepsilon\boldsymbol{I})\boldsymbol{w} \\ \text{s.t.} \quad & L \le \left|\boldsymbol{w}^{\mathrm{H}}\boldsymbol{a}(\theta)\right| \le U,\ \theta \in [\theta_L, \theta_U]. \\ & \left|\boldsymbol{w}^{\mathrm{H}}\boldsymbol{a}(\theta_k)\right| \le \xi, \quad k = 1,\ldots,K \end{aligned} \tag{13}$$

As for $\boldsymbol{w}$, $L \le |\boldsymbol{w}^{\mathrm{H}}\boldsymbol{a}(\theta)|$ is non-convex. Therefore, the optimization problem with constraint (10) cannot be solved by convex optimization method. Let $\boldsymbol{w} = \boldsymbol{w}_1 + \boldsymbol{w}_2$, when $\boldsymbol{w}_1$ is fixed, $L \le |\boldsymbol{w}^{\mathrm{H}}\boldsymbol{a}(\theta)|$ can be transformed into a SOCP problem for $\boldsymbol{w}_2$, which can be solved by convex optimization toolbox.

The constraints of optimization problem (13) can be written as

$$\begin{cases} \boldsymbol{w}^{\mathrm{H}}\boldsymbol{a}(\theta)\boldsymbol{a}^{\mathrm{H}}(\theta)\boldsymbol{w} \le U^2, & \theta \in [\theta_L, \theta_U] \\ \boldsymbol{w}^{\mathrm{H}}\boldsymbol{a}(\theta)\boldsymbol{a}^{\mathrm{H}}(\theta)\boldsymbol{w} \ge L^2, & \theta \in [\theta_L, \theta_U] \\ \boldsymbol{w}^{\mathrm{H}}\boldsymbol{a}(\theta_k)\boldsymbol{a}^{\mathrm{H}}(\theta_k)\boldsymbol{w} \le \xi^2, & k = 1,\ldots,K \end{cases}. \tag{14}$$

In order to solve the optimization problem (13), Lemma 3.1 in [23] is used as follows.

Lemma 1 For any given $\boldsymbol{a}(\theta) \in \boldsymbol{C}^M$, L and U, there exists $\boldsymbol{w} \in \boldsymbol{C}^M$ such that (15) holds if and only if there exist $\boldsymbol{w}_1 \in \boldsymbol{C}^M$ and $\boldsymbol{w}_2 \in \boldsymbol{C}^M$ such that

$$\begin{cases} (\boldsymbol{w}_1 + \boldsymbol{w}_2)^{\mathrm{H}}\boldsymbol{a}(\theta)\boldsymbol{a}^{\mathrm{H}}(\theta)(\boldsymbol{w}_1 + \boldsymbol{w}_2) \le U^2, & \theta \in [\theta_L, \theta_U] \\ 4\,\mathrm{Re}\{\boldsymbol{w}_1^{\mathrm{H}}\boldsymbol{a}(\theta)\boldsymbol{a}^{\mathrm{H}}(\theta)\boldsymbol{w}_2\} \ge L^2, & \theta \in [\theta_L, \theta_U] \\ (\boldsymbol{w}_1 + \boldsymbol{w}_2)^{\mathrm{H}}\boldsymbol{a}(\theta_k)\boldsymbol{a}^{\mathrm{H}}(\theta_k)(\boldsymbol{w}_1 + \boldsymbol{w}_2) \le \xi^2, & k = 1,\ldots,K \end{cases}. \tag{15}$$

If (15) is feasible, then $\boldsymbol{w} = \boldsymbol{w}_1 + \boldsymbol{w}_2$ is a feasible solution of (14).

For a proof, see [23]. According to Lemma 1, the optimization problem (13) can be transformed into

$$\begin{aligned}\min_{\boldsymbol{w}_2}\quad & (\boldsymbol{w}_1+\boldsymbol{w}_2)^{\mathrm{H}}(\hat{\boldsymbol{R}}+\varepsilon\boldsymbol{I})(\boldsymbol{w}_1+\boldsymbol{w}_2)\\ \text{s.t.}\quad & (\boldsymbol{w}_1+\boldsymbol{w}_2)^{\mathrm{H}}\boldsymbol{a}(\theta)\boldsymbol{a}^{\mathrm{H}}(\theta)(\boldsymbol{w}_1+\boldsymbol{w}_2)\le U^2, \quad \theta\in[\theta_L,\theta_U]\\ & 4\,\mathrm{Re}\left\{\boldsymbol{w}_1^{\mathrm{H}}\boldsymbol{a}(\theta)\boldsymbol{a}^{\mathrm{H}}(\theta)\boldsymbol{w}_2\right\}\ge L^2, \quad \theta\in[\theta_L,\theta_U]\\ & (\boldsymbol{w}_1+\boldsymbol{w}_2)^{\mathrm{H}}\boldsymbol{a}(\theta_k)\boldsymbol{a}^{\mathrm{H}}(\theta_k)(\boldsymbol{w}_1+\boldsymbol{w}_2)\le\xi^2, \quad k=1,\ldots,K\end{aligned} \tag{16}$$

If $\boldsymbol{w}_1$ is fixed, as for $\boldsymbol{w}_2$, the optimization problem (16) can be transformed into a SOCP problem. If $\boldsymbol{w}_2$is fixed, it is same for $\boldsymbol{w}_1$. According to Lemma 1, $\boldsymbol{w}_1$ is fixed, and $\boldsymbol{w}_2$ is solved by (16), and then the optimal weight vector $\boldsymbol{w}=\boldsymbol{w}_1+\boldsymbol{w}_2$ of optimization problem (13) can be obtained. However, the fixed value of $\boldsymbol{w}_1$ may not be appropriate, and the corresponding $\boldsymbol{w}=\boldsymbol{w}_1+\boldsymbol{w}_2$ may not be the optimal solution. Therefore, we modify the value of $\boldsymbol{w}_1$ in an iterative way, so as to obtain more accurate weight vector $\boldsymbol{w}=\boldsymbol{w}_1+\boldsymbol{w}_2$.

The proposed NB-DISOCP algorithm is summarized as follows.

Step 1. Obtain initial value of $\boldsymbol{w}\in\boldsymbol{C}^M$ by solving (17)

$$\begin{aligned}\min_{\boldsymbol{w}}\quad & \boldsymbol{w}^{\mathrm{H}}(\hat{\boldsymbol{R}}+\varepsilon\boldsymbol{I})\boldsymbol{w}\\ \text{s.t.}\quad & \left|\boldsymbol{w}^{\mathrm{H}}\boldsymbol{a}(\theta)-\frac{U+L}{2}\right|\le\frac{U-L}{2}, \quad \theta\in[\theta_L,\theta_U]\\ & \boldsymbol{w}^{\mathrm{H}}\boldsymbol{a}(\theta_k)\boldsymbol{a}^{\mathrm{H}}(\theta_k)\boldsymbol{w}\le\xi^2, \quad k=1,\ldots,K\end{aligned} \tag{17}$$

Let $\boldsymbol{w}_1=\boldsymbol{w}_2=\boldsymbol{w}/2$.

Step 2. Fix $\boldsymbol{w}_1$, and the optimal value of $\boldsymbol{w}_2$ can be obtained by solving (16).

Step 3. If $\|\boldsymbol{w}_1-\boldsymbol{w}_2\|\le\delta$ (δ is a constant) or the number of iterations reaches the set value, go to Step 5. Otherwise, proceed to the next step.

Step 4. Update $\boldsymbol{w}=\boldsymbol{w}_1+\boldsymbol{w}_2$ and let $\boldsymbol{w}_1=\boldsymbol{w}/2$, and then, go to Step 2.

Step 5. Obtain the optimal weight vector $\boldsymbol{w}=\boldsymbol{w}_1+\boldsymbol{w}_2$.

The computational complexity of the proposed method is dominated by solving the SOCP problem. Therefore, the computational complexity of the proposed method is $O(M^{3.5})$, and it is comparable to other robust beamforming algorithms.

4. Simulation Results

In our simulations, the parameter setting is consistent with the existing reference [13, 19, 20]. The experimental results are all obtained by Monte Carlo simulation in MATLAB 7.11 environment, and the algorithms involving convex optimization are solved by CVX toolbox [24]. A uniform linear array of $M = 10$ omnidirectional sensors spaced half a wavelength is considered. The noise is Gaussian white noise with zero mean and unit variance. Assume that the DS impinges on the array from 0°, the input SNR is 0 dB, and the number of snapshots is $N = 100$.The two interference signals impinge on the array from –40° and 50° respectively, and the interference-to-noise ratio (INR) is 30 dB. The proposed NB-DISOCP beamformer is compared with the following beamformers: the sample matrix inversion (SMI) beamformer (8), the eigenspace-based (EIG) beamformer [6], the RCB [7], the CMT method [13], the PDL approach [20], and the LCSS algorithm [19]. For a given ripple level r_{dB} (dB), L and U are taken as $L=10^{-r_{\mathrm{dB}}/20}$ and $U=10^{r_{\mathrm{dB}}/20}$, respectively. For the null broadening methods CMT, PDL, LCSS, and NB-DISOCP, the null width is set to be 10°, that is, the angular sectors of the interferences are $[-45°,-35°]\cup[45°,55°]$. The uncertainty set parameter of the RCB is assumed to be $\varepsilon = 0.3M$ [4]. The number of base vectors of PDL is taken as $L = 6$, and the diagonal loading factor is set to be $\lambda = 0.01$ [20]. In the LCSS beamformer, the pre-specified suppression level is taken as $\eta = 10^{-7}$. In the NB-DISOCP beamformer, the angular sector of mainlobe is assumed to be $[-5°,5°]$, and the ripple level is $r_{\mathrm{dB}} = 0.3$ dB, $\varepsilon_{\mathrm{r}} = 0.1$, $\xi^2 = 10^{-7}$. For each scenario, 100 Monte Carlo runs are performed.

4.1 Impact of the Number of Iterations on the Performance of the NB-DISOCP Algorithm

In the first example, the impact of the number of iterations on the performance of the NB-DISOCP algorithm is examined. Figure 1 shows the beampattern of the NB-DISOCP algorithm under different iteration times. It can be observed that the beampatterns under the 4th iteration and the 10th iteration are similar, and the beampatterns under the 10th iteration and the 15th iteration are almost overlapped, indicating that the NB-DISOCP algorithm basically converges under the 4th iteration. Figure 2 displays the output SINR of the NB-DISOCP algorithm versus the number of iterations. As the number of iterations increases, the output SINR increases, and it basically converges under

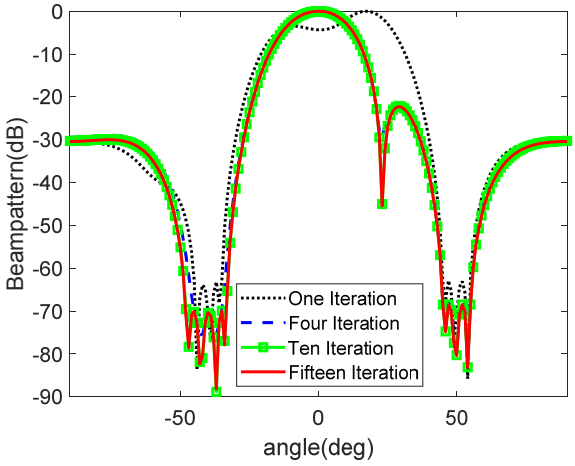

Fig. 1. Beampattern of the NB-DISOCP algorithm under different iteration times.

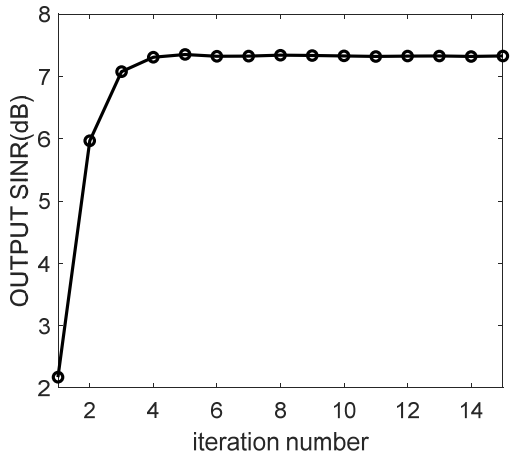

Fig. 2. Output SINR of the NB-DISOCP algorithm versus the number of iterations.

converges under the 4th iteration. Therefore, the NB-DISOCP iterative algorithm can effectively converge.

4.2 Performance of Null Broadening

In the second example, the normalized beampattern is examined to compare the performance of the null broadening. Figure 3 illustrates the normalized beampattern of these approaches, and the normalized beampattern at –40° is shown in Fig. 4. It can be seen from these figures that the nulls of the NB-DISOCP approach are wider than those of other approaches, which can better suppress non-stationary interference. In addition, the NB-DISOCP also widens the mainlobe to form a flat-topped mainlobe, which improves the robustness to SV mismatch with a small loss of antenna gain. At the same time, it reduces the sidelobe levels, and the average value of the sidelobe levels on both sides is about –30 dB. Consequently, NB-DISOCP demonstrates good performance of beamforming. In order to more intuitively compare the null broadening performance of these approaches, null widths of different gains at –40° are reported in Tab. 1. As shown from Tab. 1, the null of CMT is the shallowest. The NB-DISOCP and LCSS can still broaden

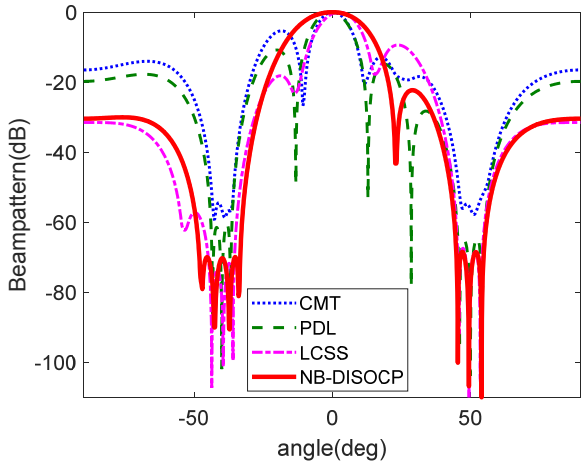

Fig. 3. Normalized beampattern.

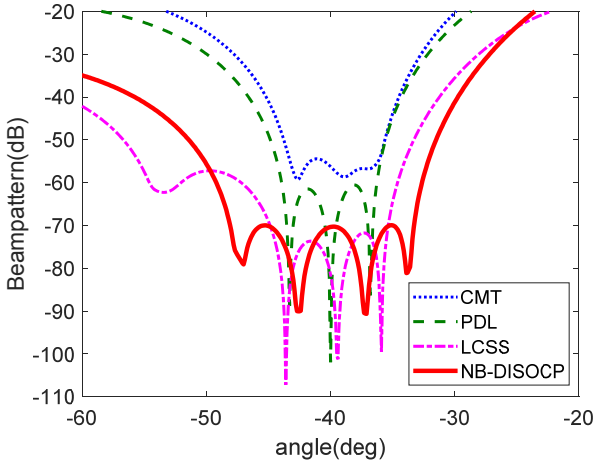

Fig. 4. Null broadening effect at –40°.

Beamformer	Gain		
	–50 dB	–60 dB	–70 dB
CMT	8.2°	-	-
PDL	9.2°	7.6°	-
LCSS	23.4°	12.6°	9.8°
NB-DISOCP	19.9°	16.6°	14.8°

Tab. 1. Null width of different gains at –40°.

the null at the gain of –70 dB. At this time, the null width of the NB-DISOCP is the widest, which is about 14.8°. Therefore, NB-DISOCP has good performance of null broadening and beamforming, and it attributes the success to the mainlobe and null constraints in the model.

4.3 Mismatch Due to Signal Look Direction Error

In the third example, we show the impact of signal look direction error on the output SINR. Figure 5 reveals the output SINR versus the pointing error for SNR = 20 dB. It can be observed from the figure that the output SINR of the NB-DISOCP remains unchanged versus pointing error, and it has good performance under both large and small signal pointing error. Although the output SINR of the PDL under the small signal pointing error is higher than that of the NB-DISOCP, when the pointing error is greater than 7°, the performance of the PDL will severely degrade. The output SINR of other approaches tested is much lower than that of the NB-DISOCP and PDL. Figure 6 depicts the output SINR versus the input SNR when the signal pointing error is 7°. As shown in the figure, when the signal pointing error is 7°, the output SINR of the PDL and NB-DISOCP is high in a large range of input SNR, and they can still maintain a good performance with high input SNR. Moreover, the output SINR of the NB-DISOCP is better than that of the PDL. The output SINR of other approaches tested will decrease with high input SNR. In the proposed method, we control the mainlobe beamwidth in a large region and mainlobe ripple in a small region. Therefore, the NB-DISOCP has good robustness to SV mismatch, especially large SV mismatch.

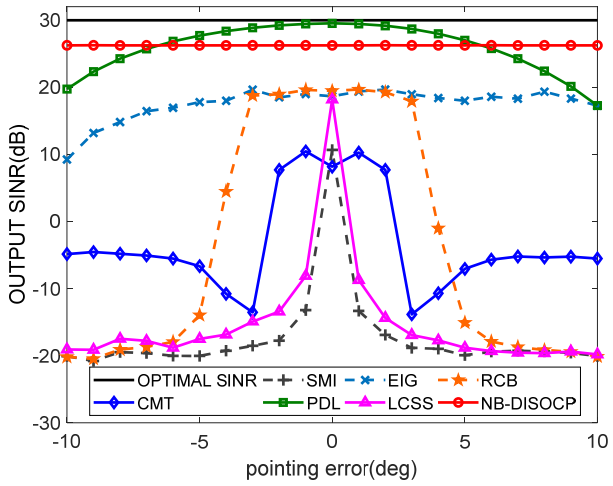

Fig. 5. Output SINR versus pointing error.

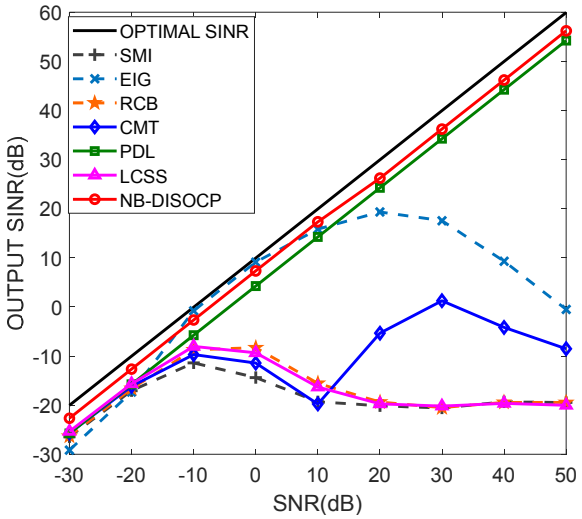

Fig. 6. Output SINR versus input SNR when the signal pointing error is 7°.

4.4 Mismatch Due to Signal Look Direction Error and Non-stationary Interference

In the last example, we simulate the situation when there exist both signal look direction error and non-stationary interference. Assume that the actual DS impinges on the array from 0° with a 7° mismatch in the signal look direction. Figure 7 describes the output SINR versus the deviation of interference arrival direction when both the signal look direction error and non-stationary interference exist. From the figure, we can see that the SMI, EIG, and RCB are not robust against non-stationary interference because they do not broaden the nulls, and the output SINR of them decreases as the deviation of interference arrival direction increases. The output SINR of the CMT, PDL, LCSS, and NB-DISOCP decreases when the deviation of interference arrival direction reaches 4°, 5°, 6°, and 7°, respectively. And the output SINR of the NB-DISOCP is better than others. Therefore, the NB-DISOCP has the strongest robustness when signal look direction error and non-stationary interference exist simultaneously. In Fig. 8 and Fig. 9, the directions of the two interference signals are random and uniformly distributed in $[-45°,-35°] \cup [45°,55°]$, and the DOAs of the interference signals change from run to run while remaining fixed from snapshot to snapshot. Figure 8 exhibits the output SINR versus the input SNR when both the signal look direction error and non-stationary interference exist. As shown in the figure, the output SINR of the NB-DISOCP is the highest and is relatively close to the optimal SINR. Furthermore, the NB-DISOCP can still maintain a high output SINR under the high input SNR. The output SINR of the PDL is inferior to that of the NB-DISOCP, and the output SINR of the SMI, EIG, RCB, CMT, and LCSS decreases seriously with the increase of the input SNR. Therefore, the NB-DISOCP has strong joint robustness to SV mismatch and non-stationary interference in a large input SNR range. Figure 9 displays the output SINR versus the number of snapshots when the signal look direction error and non-stationary interference exist simultaneously.

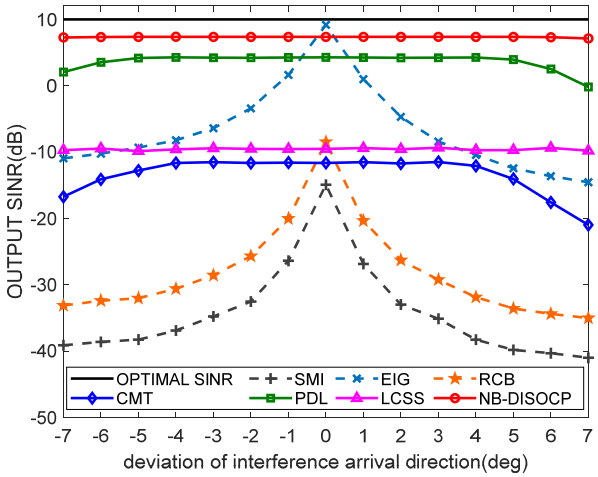

Fig. 7. Output SINR versus deviation of interference arrival direction when the signal look direction error and non-stationary interference exist simultaneously.

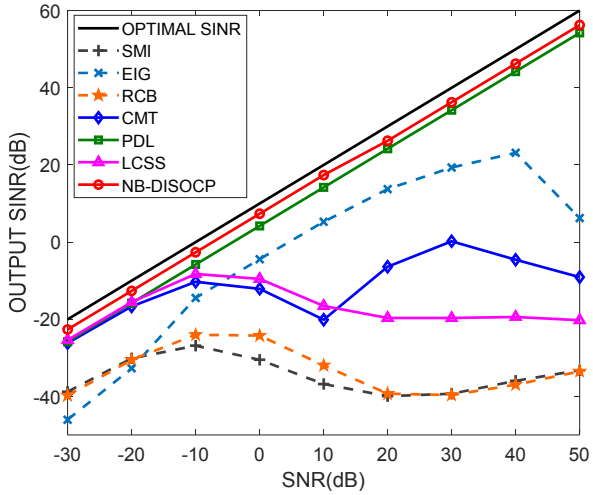

Fig. 8. Output SINR versus input SNR when the signal look direction error and non-stationary interference exist simultaneously.

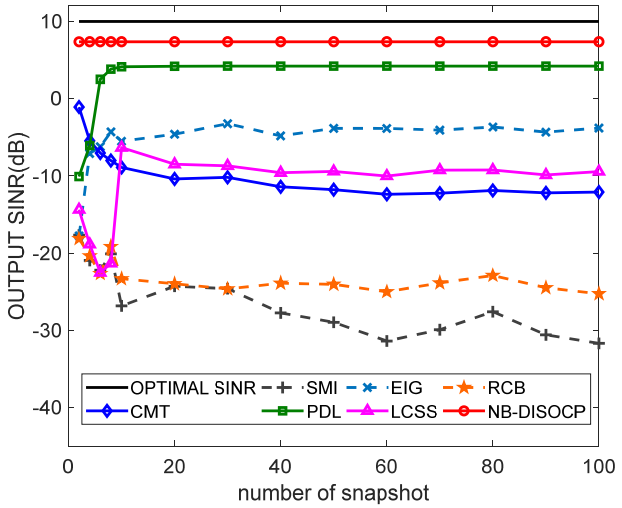

Fig. 9. Output SINR versus number of snapshots when the signal look direction error and non-stationary interference exist simultaneously.

It can be observed that the performance of most algorithms is affected when the number of snapshots is lower than the number of array elements, while the output SINR of the NB-DISOCP remains unchanged, indicating that the NB-DISOCP can still work effectively in the condition of low snapshot. In summary, the NB-DISOCP has good joint robustness to SV mismatch and non-stationary interference. Readers interested in this article can refer to the relevant source code from the link in footnote.[1]

5. Conclusions

In order to improve the robustness of the beamformer when the SV mismatch and non-stationary interference exist simultaneously, a null broadening robust beamforming algorithm based on the decomposition and iterative second-order cone programming is proposed in this paper. The algorithm constrains the magnitude of the mainlobe and the depth of the null respectively, and then converts the non-convex optimization problem into an iterative second-order cone programming problem to solve. Simulation results demonstrate that the proposed algorithm has joint robustness to SV mismatch and non-stationary interference, and it can still work effectively in the case of low snapshot. In future, we will study the other method which is based on first-order Taylor expansion to solve the proposed model.

Acknowledgments

This work was supported by the National Natural Science Foundation of China under grant 62001500.

[1]https://github.com/jinweimail/code-for-NB-DISOCP.git

References

[1] VOROBYOV, S. A. Principles of minimum variance robust adaptive beamforming design. *Signal Processing*, 2013, vol. 93, no. 12, p. 3264–3277. DOI: 10.1016/j.sigpro.2012.10.021

[2] ZHU, X., XU, X., YE, Z. Robust adaptive beamforming via subspace for interference covariance matrix reconstruction. *Signal Processing*, 2020, vol. 167, p. 1–10. DOI: 10.1016/j.sigpro.2019.107289

[3] JIN, W., JIA, W. M., ZHANG, F. G., et al. A user parameter-free robust adaptive beamformer based on general linear combination in tandem with steering vector estimation. *Wireless Personal Communications*, 2014, vol. 75, no. 2, p. 1447–1462. DOI: 10.1007/s11277-013-1432-1

[4] VOROBYOV, S. A., GERSHMAN, A. B., LUO, Z. Q. Robust adaptive beamforming using worst-case performance optimization: a solution to the signal mismatch problem. *IEEE Transactions on Signal Processing*, 2003, vol. 51, no. 2, p. 313–324. DOI: 10.1109/tsp.2002.806865

[5] CARLSON, B. D. Covariance matrix estimation errors and diagonal loading in adaptive arrays. *IEEE Transactions on Aerospace and Electronic Systems*, 1988, vol. 24, no. 4, p. 397–401. DOI: 10.1109/7.7181

[6] FELDMAN, D. D., GRIFFITHS, L. J. A projection approach for robust adaptive beamforming. *IEEE Transactions on Signal Processing*, 1994, vol. 42, no. 4, p. 867–876. DOI: 10.1109/78.285650

[7] LI, J., STOICA, P., WANG, Z. S. On robust Capon beamforming and diagonal loading. *IEEE Transactions on Signal Processing*, 2003, vol. 51, no. 7, p. 1702–1715. DOI: 10.1109/tsp.2003.812831

[8] GU, Y., LESHEM, A. Robust adaptive beamforming based on interference covariance matrix reconstruction and steering vector estimation. *IEEE Transactions on Signal Processing*, 2012, vol. 60, no. 7, p. 3881–3885. DOI: 10.1109/tsp.2012.2194289

[9] HASSANIEN, A., VOROBYOV, S. A., WONG, K. M. Robust adaptive beamforming using sequential quadratic programming: An iterative solution to the mismatch problem. *IEEE Signal Processing Letters*, 2008, vol. 15, p. 733–736. DOI: 10.1109/lsp.2008.2001115

[10] JIN, W., JIA, W. M., YAO, M. L., et al. A robust adaptive beamforming algorithm using decomposition and iterative second-order cone programming. *Journal of Electronics and Information Technology*, 2012, vol. 34, no. 9, p. 2051–2057. (In Chinese) DOI: 10.3724/SP.J.1146.2012.00146

[11] MAILLOUX, R. J. Covariance matrix augmentation to produce adaptive array pattern troughs. *Electronics Letters*, 1995, vol. 31, no. 10, p. 771–772. DOI: 10.1049/el:19950537

[12] ZATMAN, M. Production of adaptive array troughs by dispersion synthesis. *Electronics Letters*, 1995, vol. 31, no. 25, p. 2141–2142. DOI: 10.1049/el:19951486

[13] GUERCI, J. R. Theory and application of covariance matrix tapers for robust adaptive beamforming. *IEEE Transactions on Signal Processing*, 1999, vol. 47, no. 4, p. 977–985. DOI: 10.1109/78.752596

[14] GERSHMAN, A. B., NICKEL, U., BOHME, J. F. Adaptive beamforming algorithms with robustness against jammer motion. *IEEE Transactions on Signal Processing*, 1997, vol. 45, no. 7, p. 1878–1885. DOI: 10.1109/78.599965

[15] GERSHMAN, A. B., SEREBRYAKOV, G. V., BOHME, J. F. Constrained Hung-Turner adaptive beam-forming algorithm with additional robustness to wideband and moving jammers. *IEEE Transactions on Antennas and Propagation*, 1996, vol. 44, no. 3, p. 361–367. DOI: 10.1109/8.486305

[16] ZATMAN, M. Comments on "Theory and application of covariance matrix tapers for robust adaptive beamforming". *IEEE Transactions on Signal Processing*, 2000, vol. 48, no. 6, p. 1796–1800. DOI: 10.1109/78.845937

[17] LIU, F. L., CHEN, P. P., WANG, J. K., et al. Null broadening and sidelobe control method based on multi-parametric quadratic programming. *Journal of Northeastern University*, 2012, vol. 33, no. 11, p. 1559–1562. (In Chinese) DOI: 1005-3026(2012)33:11<1559:JYDCSE>2.0.TX;2-3

[18] ER, M. H. Technique for antenna array pattern synthesis with controlled broad nulls. *IEE Proceedings*, 1988, vol. 135, no. 6, p. 375–380. DOI: 10.1049/ip-h-2.1988.0079

[19] AMAR, A., DORON, M. A. A linearly constrained minimum variance beamformer with a pre-specified suppression level over a pre-defined broad null sector. *Signal Processing*, 2015, vol. 109, p. 165–171. DOI: 10.1016/j.sigpro.2014.11.009

[20] MAO, X. J., LI, W. X., LI, Y. S., et al. Robust adaptive beamforming against signal steering vector mismatch and jammer motion. *International Journal of Antennas and Propagation*, 2015, p. 1–12. DOI: 10.1155/2015/780296

[21] QIAN, J., HE, Z., XIE, J., et al. Null broadening adaptive beamforming based on covariance matrix reconstruction and similarity constraint. *EURASIP Journal on Advances in Signal Processing*, 2017, p. 1–10. DOI: 10.1186/s13634-016-0440-1

[22] MOHAMMADZADEH, S., KUKRER, O. Robust adaptive beamforming for fast moving interference based on the covariance matrix reconstruction. *IET Signal Processing*, 2019, vol. 13, no. 4, p. 486–493. DOI: 10.1049/iet-spr.2018.5264

[23] WANG, F., BALAKRISHNAN, V., ZHOU, P. Y., et al. Optimal array pattern synthesis using semidefinite programming. *IEEE Transactions on Signal Processing*, 2003, vol. 51, no. 5, p. 1172–1183. DOI: 10.1109/tsp.2003.810308

[24] GRANT, M., BOYD, S. Cvx users' guide for cvx version 1.2. 2009. Available at: http://www.stanford.edu/~boyd/cvx.html

About the Authors ...

Wei JIN (corresponding author) was born in Hubei, China in 1984. He received his Ph.D. degree from the Xi'an Research Institute of High Technology, Xi'an, China, in 2013. He is an Associate Professor in the Xi'an Research Institute of High Technology. At present, he is doing post-doctoral work in the National Laboratory of Radar Signal Processing, Xidian University, Xi'an, China. His research interests include the array signal processing and radar signal processing.

Yunzhou GUO was born in Shaanxi, China in 1995. She is studying for her M.Sc. from the Xi'an Research Institute of High Technology, Xi'an, China. Her research interests include the array signal processing and robust adaptive beamforming.

Weimin JIA was born in Hebei, China in 1971. She received her Ph.D. degree from the Xi'an Research Institute of High Technology, Xi'an, China, in 2007. She is a Professor in the Xi'an Research Institute of High Technology. Her research interests include the Sat-COM and smart antennas.

Jianwei ZHAO was born in Shandong, China in 1989. He received his Ph.D. degree from the Xi'an Research Institute of High Technology, Xi'an, China, in 2019. He is a lecturer in the Xi'an Research Institute of High Technology. His research interests include massive MIMO systems and unmanned aerial vehicle communication systems.